Supporting Information

Cleary et al. 10.1073/pnas.1218270110

SI Materials and Methods

Model of *N*-Fold Geometry. To study the effect of the fold symmetry on the optimal rotational configuration we construct a model N-fold geometry. The configuration of each heterodimer is independent of the fold number N, so that we may fix the $\alpha\beta$-heterodimer structure (1). As indicated in Fig. S1, this subunit of light-harvesting complex 2 (LH2) consists of two B850 bacterichlorophylls (BChls). Between the two B850 BChls within the heterodimer the Mg–Mg distance is set to $a = 9.45$ Å, whereas between the nearest BChls of neighboring heterodimers, the Mg–Mg distance is set to $b = 9.01$ Å. The orientations of the heterodimer's transition dipole moments, taken with relation to the Mg–Mg vector within the heterodimer, are $\theta_\alpha = 168.63°$ and $\theta_\beta = -21.06°$. We have obtained these values from the LH2 B850 ring structure of *Rhodopseudomonas acidophila* (Protein Data Bank ID 1NKZ).

Next, we assume that an N-fold ring may be constructed by mapping this fixed-structure heterodimer N times around a single circumference. Due to this constraint, both the radius, R, and the angle, α, subtended at the origin by the cord a, are explicit functions of the fold number N and heterodimer constants a and b. From Fig. S1, we obtain the relations

$$R\,\sin(\alpha/2) = a/2,$$

$$R\,\sin[(2\pi/N - \alpha)/2] = b/2.$$

Solving the above simultaneous equations yields

$$\alpha = 2\,\sin^{-1}(a/2R),$$

and

$$R = \frac{\sqrt{a^2 + b^2 + 2ab\,\cos(\pi/N)}}{2\,\sin(\pi/N)}. \qquad \textbf{[S1]}$$

Eq. **S1** is the radius of the N-fold B850 ring subject to the constraints of a fixed dimer structure aligned upon a single circumference. For $N = 8$ and $N = 9$ Eq. **S1** yields radii of 23.67 Å and 26.59 Å, which compare favorably with the radii of *Rhodospirillum molischianum* and *Rps. acidophila*, 23.4 Å and 26.37 Å, respectively.

Model Hamiltonian. In the site basis, the system Hamiltonian of a single B850 ring with N-fold symmetry is (2)

$$H = \sum_{n=1}^{2N} E_n |n\rangle\langle n| + \sum_{n \neq n'}^{2N} V_{nn'} |n\rangle\langle n'|, \qquad \textbf{[S2]}$$

where $|n\rangle$ represents the state where only the nth chromophore is in its excited state and all others are in their ground states (3). E_n is the site energy of the nth chromophore, defined as the optical transition energy at the equilibrium configuration of environmental phonons associated with the ground state. $V_{nn'}$ denotes the electronic coupling between the nth and the n'th chromophores and is responsible for migration of electronic excitation within the complex. The non-nearest-neighbor coupling terms are calculated using the dipole–dipole approximation $V_{nn'} = C[(\vec{d}_n \cdot \vec{d}_{n'})/|\vec{r}_{nn'}|^3 - 3(\vec{r}_{nn'} \cdot \vec{d}_{n'})(\vec{r}_{nn'} \cdot \vec{d}_n)/|\vec{r}_{nn'}|^5]$, where $\vec{d}_n = \langle 0|\hat{\mu}|n\rangle$ is a unit vector describing the direction of the dipole moment of the ground state $|0\rangle$ to the Q_y excited state transition of the nth chromophore, $\hat{\mu}$ is the dipole operator, $\vec{r}_{nn'}$ is the vector connecting the centers of chromophore n and chromophore n', and C is an appropriate, dimensioned constant. The following values are used throughout: the site energy $E_n = 12480$ cm^{-1}, the intradimer coupling $V_{2n-1,2n} = V_{2n,2n-1} = 363$ cm^{-1} $(n = 1, \ldots N)$, the interdimer coupling $V_{2n+1,2n} = V_{2n,2n+1} = V_{1,2N} = V_{2N,1} = 320$ cm^{-1} $(n = 1, \ldots N-1)$, and the dimensioned constant $C = 348{,}000$ Å^3·cm^{-1} (4, 5). Note that we have neglected the dependence of the interdimer coupling on the fold number N (due to the changing orientations of the neighboring transition dipole vectors). This is of no consequence to our results and conclusions.

An important property of N-fold symmetric ring structures is the existence of $N-2$ and $N-1$ pairs of degenerate eigenstates for even and odd N, respectively (6). Consider the dimeric (N-fold) structure of the B850 ring. One can introduce the column vector $|.\rangle\rangle$ of local states

$$|p\rangle\rangle = \begin{pmatrix} |2p-1\rangle \\ |2p\rangle \end{pmatrix}, \qquad \textbf{[S3]}$$

where $p = 1, 2, \ldots N$, and the 2×2 matrix of coupling terms

$$H_{qp} = \begin{pmatrix} V_{2q-1,2p-1} & V_{2q-1,2p} \\ V_{2q,2p-1} & V_{2q,2p} \end{pmatrix}, \qquad \textbf{[S4]}$$

with $V_{qq} = E_q$, so that the Hamiltonian Eq. **S2** may be written $H = \sum_{q,p}^{N} H_{qp} |q\rangle\rangle\langle\langle p|$. Due to the periodicity of the ring, the eigenvector coefficients of this Hamiltonian are simply the Fourier coefficients, i.e., ref. 6,

$$|k\rangle\rangle = \frac{1}{\sqrt{N}} \sum_{p=1}^{N} e^{ik(2\pi p/N)} |p\rangle\rangle, \qquad \textbf{[S5]}$$

where $k = 1, 2, \ldots N$. The corresponding eigenvalues are

$$\langle\langle k|H|k\rangle\rangle = \frac{1}{N} \sum_{q=1,p=1}^{N} e^{ik2\pi(p-q)/N} H_{qp} = \sum_{p=2}^{N} e^{ik2\pi(p-1)/N} H_{1p}. \qquad \textbf{[S6]}$$

According to Eq. **S6**, when N is even, there are two nondegenerate states $k = N/2$ and $k = N$ as well as $(N-2)/2$ pairs of degenerate states $k = j$ and $k = N - j$, $[j = 1, 2, \ldots (N/2 - 1)]$. For odd N, the spectrum consists of only one nondegenerate state, $k = N$, and $(N-1)/2$ pairs of degenerate states, $k = j$ and $k = N - j, [j = 1, 2, \ldots (N-1)/2]$. However, the above analysis is for the "monomer" case. Each LH2 site is a dimer. Thus, diagonalization of each dimer-Hamiltonian H_{1p} yields an eigenenergy splitting, which gives rise to two subeigenenergies. As a result, we get $2 \times 2 = 4$ nondegenerate states and $2 \times (N-2)/2 = N-2$ pairs of degenerate states for even N, as well as $2 \times 1 = 2$ nondegenerate states and $2 \times (N-1)/2 = N-1$ pairs of degenerate states for odd N. For example, for $N = 8$ diagonalization of the Hamiltonian (2) yields four nondegenerate eigenstates $|\varepsilon_1\rangle, |\varepsilon_8\rangle, |\varepsilon_9\rangle$, and $|\varepsilon_{16}\rangle$, as well as six pairs of degenerate eigenstates. Similarly, a fold number of $N = 9$ yields two nondegenerate eigenstates $|\varepsilon_1\rangle$ and $|\varepsilon_{18}\rangle$, as well as eight pairs of degenerate eigenstates. From this analysis, it is clear that the eigenenergy structure of an LH2 B850 ring is decided by the fold symmetry number N arising from the dimeric structure of the ring.

Mirror Symmetry Lines of Two *N*-Fold Rings. The excitation energy transfer (EET) rate between two N-fold rings as a function of the rotation angles, $|J|^2_{12} \equiv F(\theta_1, \theta_2)$, displays mirror symmetry lines at $\theta_1 = \theta_2 \pm \pi/9$ for $N = 9$ and a symmetry line at $\theta_1 = \theta_2$ for $N = 8$ (dashed lines in Fig. 3*A* and Fig. S3*A*, respectively). Using a simple geometrical argument, we prove that the phase shift of the mirror symmetry lines $\phi_N = \theta_1 - \theta_2 + 2\pi p/N$, $(p \in \mathbb{Z})$ for any N is

$$\phi_N = \begin{cases} \pi/N & N \text{ odd}, \\ 0 & N \text{ even}. \end{cases} \qquad \textbf{[S7]}$$

For odd fold numbers, consider the EET rate between two three-fold rings. As shown in Fig. S2*A*, the initial rotational configuration is given by (θ_1, θ_2). If we rotate the whole system by 180° (C_2 rotation) about the point O, it is easy to see that the new configuration in Fig. S2*B* is given by $(\theta_2 + \pi, \theta_1 + \pi)$. However, the EET rate $F(\theta_1, \theta_2)$ between the two rings is invariant under C_2 rotation of the whole system. Hence we have

$$\begin{aligned} F(\theta_1, \theta_2) &= F(\theta_2 + \pi, \theta_1 + \pi), \\ &= F(\theta_2 + \pi/3, \theta_1 + \pi/3), \end{aligned}$$

where the second relation follows from the $2\pi/3$ periodicity of the individual rings. We thus have identified the point (θ_1, θ_2) with $(\theta_2 + \pi/3, \theta_1 + \pi/3)$ on the EET landscape F. This is exactly equivalent to having mirror symmetry lines at $\theta_1 = \theta_2 \pm \pi/3$. This argument is easily generalized to any odd N, providing a simple proof of Eq. **S7** for N odd.

For even fold numbers, because π is always evenly divisible by the ring's periodicity $2\pi/N$, one obtains the result $F(\theta_1, \theta_2) = F(\theta_2 + \pi, \theta_1 + \pi) = F(\theta_2, \theta_1)$ so that the mirror symmetry line is $\theta_1 = \theta_2$. This provides proof of Eq. **S7** for N even.

1. Janosi L, Keer H, Kosztin I, Ritz T (2006) Influence of subunit structure on the oligomerization state of light-harvesting complexes: A free energy calculation study. *Chem Phys* 323(1):117–128.
2. Davydov AS (1962) *Theory of Molecular Excitons* (Plenum, New York).
3. Renger T, May V, Kühn O (2001) Ultrafast excitation energy transfer dynamics in photosynthetic pigment–protein complexes. *Phys Rep* 343:137–254.
4. Hu X, Ritz T, Damjanović A, Schulten K (1997) Pigment organization and transfer of electronic excitation in the photosynthetic unit of purple bacteria. *J Phys Chem B* 101(19):3854–3871.
5. Strümpfer J, Schulten K (2009) Light harvesting complex II B850 excitation dynamics. *J Chem Phys* 131(22):225101.
6. Hochstrasser RM (1966) *Molecular Aspects of Symmetry* (W A Benjamin, New York).

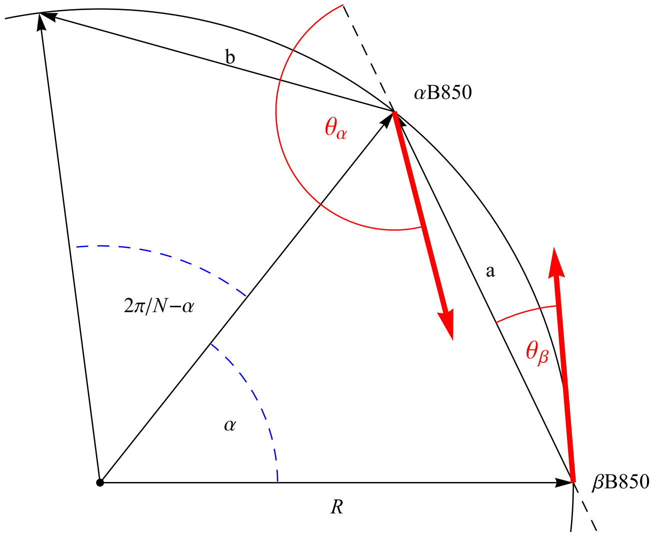

Fig. S1. Model of *N*-fold geometry. The structure of a single $\alpha\beta$-heterodimer subunit is fixed by specifying the intradimer Mg–Mg distance $a = 9.45$ Å and interdimer Mg–Mg distance $b = 9.01$ Å. The orientations of the transition dipole moments are $\theta_\alpha = 168.63°$ and $\theta_\beta = -21.06°$. The radius R and angle α are explicit functions of the fold number N and constants a and b.

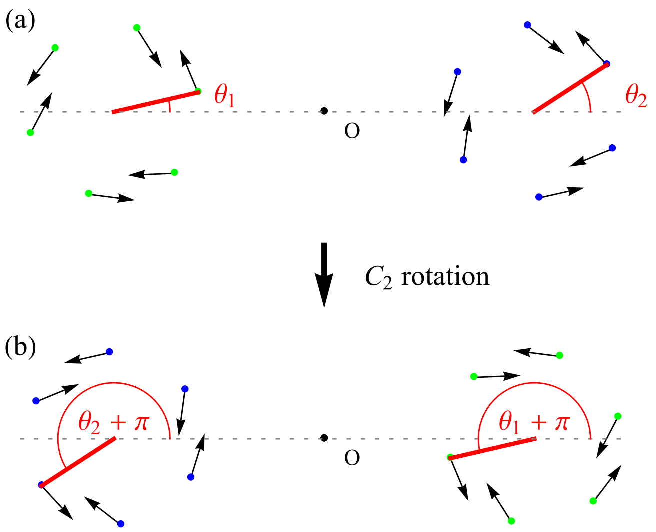

Fig. S2. (*A*) EET landscape $F(\theta_1, \theta_2)$ of a pair of *N*-fold rings is invariant under C_2 rotation about the point *O* of the two rings. (*B*) Consequently $F(\theta_1, \theta_2) = F(\theta_2 + \pi, \theta_1 + \pi)$.

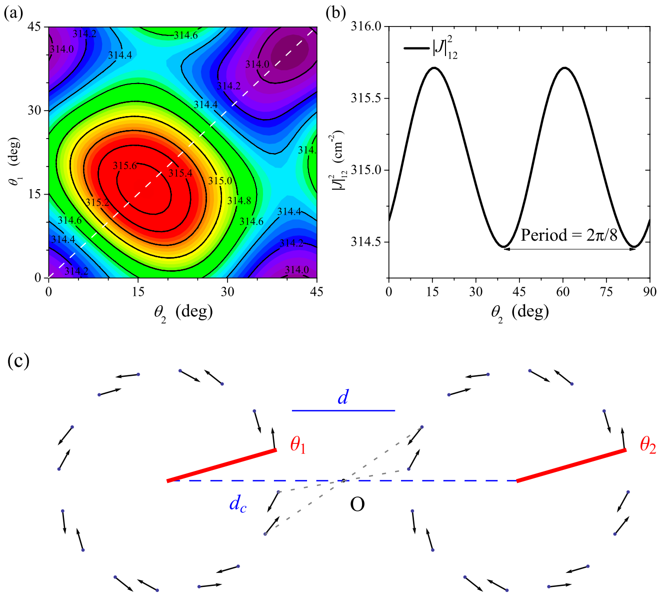

Fig. S3. (*A*) EET rate surface $|J|^2_{12}$ between two eightfold B850 rings as a function of the rotation angles θ_1 and θ_2. The mirror symmetry line $\theta_1 = \theta_2$ is indicated by the dashed line and passes through the maximum at $\theta_1 = \theta_2 = 16°$. (*B*) Cross section of the surface in *A* for $\theta_1 = 16°$, showing the $2\pi/8$ periodicity. (*C*) Optimal rotational configuration has both rotational and point symmetry about and through the point *O*.

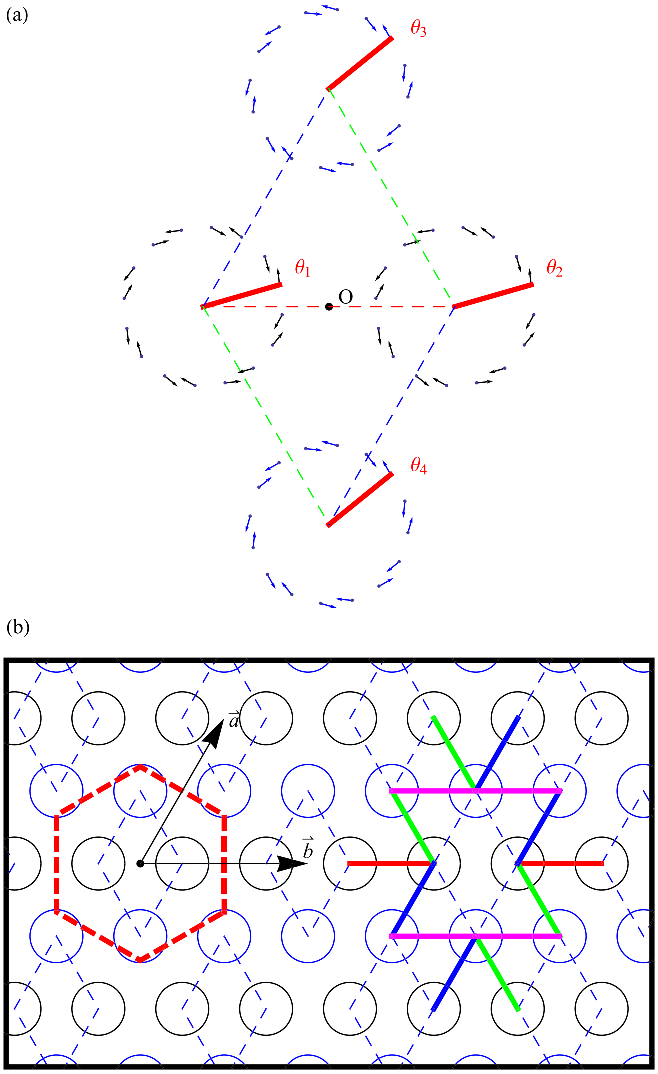

Fig. S4. (*A*) Four eightfold B850 rings placed at the vertices of a rhombus basis cell (dashed line). The matching EET rates (indicated by color) are $|J|^2_{23} = |J|^2_{14}$ and $|J|^2_{31} = |J|^2_{42}$ and the rotation angles are $\theta_1 = \theta_2 = 16^\circ$ and $\theta_3 = \theta_4 = 39^\circ$. Consequently the optimal rotational configuration has rotational symmetry of order 2 with respect to the central point *O*. (*B*, *Left*) Primitive unit cell of the Bravais lattice (thick dashed line), where $\vec{a}$ and $\vec{b}$ are the primitive vectors that generate the lattice. (*B*, *Right*) Boundary rates (14 thick solid lines) of the rhombus basis cell (colors indicate rates of equal magnitude).